J. Plasma Physics (1999), *vol.* 62, *part* 2, *pp.* 233–248 Printed in the United Kingdom
© 1999 Cambridge University Press

Dispersion in an intrinsically relativistic, one-dimensional, strongly magnetized pair plasma

D. B. MELROSE,[1] M. E. GEDALIN,[2] M. P. KENNETT[1] and C. S. FLETCHER[1,3]

[1] Research Centre for Theoretical Astrophysics, School of Physics, University of Sydney, NSW 2006, Australia
[2] Department of Physics, Ben Gurion University of the Negev, Beer Sheva 84105, Israel
[3] Department of Physics, University of Western Australia, Nedlands, WA 6907, Australia

(Received 8 December 1998 and in revised form 18 March 1999)

Abstract. The properties of a relativistic plasma dispersion function (RPDF) for an intrinsically extremely relativist, strongly magnetized, one-dimensional, electron–positron plasma are discussed in detail. For a plasma with a mean Lorentz factor $\langle\gamma\rangle \gg 1$ in its rest frame, the RPDF has a large peak $> \langle\gamma\rangle$ at a phase speed a fraction of order $1/\langle\gamma\rangle$ below the speed of light, and the asymptotic value (infinite phase speed) is $\langle\gamma^{-3}\rangle \sim 1/\langle\gamma\rangle$. These features are not particularly sensitive to the choice of distribution function. The RPDF is used to discuss the properties of waves in such plasmas. Particular points discussed are the implications of the RPDF for the maximum frequency for parallel Langmuir waves, and for the reconnection between the Langmuir mode and the Alfvén mode.

1. Introduction

The plasma in the source region of radio emission in polar-cap models for pulsars (see e.g. Ruderman and Sutherland 1975) is thought to be an intrinsically extremely relativistic, strongly magnetized, one-dimensional, electron–positron pair plasma. There is an extensive literature on the properties of waves in such a plasma (see e.g. Tsytovich and Kaplan 1972; Godfrey et al. 1975a; Suvorov and Chugunov 1975; Hardee and Rose 1976; Melrose and Stoneham 1977; Lominadze et al. 1979; Allen and Melrose 1982; Gedalin and Machabeli 1983; Volokitin et al. 1985; Asséo et al. 1983; Arons and Barnard 1986; Beskin et al. 1988; Lyutikov 1998). Various simplifying assumptions have been made in treating the wave dispersion. One specific approximation, which we make throughout, is that the wave frequencies of interest are well below the (relativistic) gyrofrequencies of the particles; however, we do not make the infinite-B approximation (in which this ratio is set to zero and the Alfvén speed is assumed infinite), which is too extreme in that it precludes a discussion of the dispersion of Alfvén and magnetoacoustic waves. Other approximations that have been made in much of the earlier literature are that the plasma in its rest frame is either cold (see e.g. Godfrey et al. 1975a; Hardee and Rose 1976; Melrose and Stoneham 1977; Allen and Melrose 1982; see also von Hoensbroech et al. 1998) or nonrelativistic (e.g., Weatherall 1994). Such approximations are equivalent to assuming that the only relativistic effect included is a streaming motion, which may be removed by a Lorentz

https://doi.org/10.1017/S0022377899007795 Published online by Cambridge University Press

transformation. Such assumptions avoid the need to consider a relativistic plasma dispersion function (RPDF). However, the spread in particle energies in a pulsar plasma is thought to be extremely relativistic (see e.g. Daugherty and Harding 1983), so that an intrinsically relativistic treatment is needed. For some purposes, the use of an RPDF can be avoided by appealing to moments of the distribution function to determine important features of the wave properties (see e.g. Lominadze and Mikhailovskii 1979; Lominadze et al. 1979; Volokitin et al. 1985), but there are important features of the wave properties for which the introduction of a RPDF is essential. In particular, an adequate treatment of the dispersion of parallel, subluminal Langmuir waves requires an RPDF. These wave properties are of particular interest in favoured pulsar radio emission mechanisms in which Langmuir waves are assumed to be generated through a beam instability (see e.g. Asséo and Melikidze 1998, and references therein).

In this paper, our main purpose is to discuss the properties of a relevant RPDF for an intrinsically extremely relativistic, strongly magnetized, one-dimensional, electron–positron pair plasma. We illustrate some of the implications of the RPDF by applying it to a discussion of wave properties in a pulsar plasma. The definition of an RPDF depends on the distribution function of the particles, which we write as $f(u)$, in terms of the parameter $u = p/m$, where p is the momentum, so that the Lorentz factor is $\gamma = (1+u^2)^{1/2}$ and the speed is $v = u/\gamma$ (units with $c = 1$ are used throughout). Different choices of distribution function have been made in the literature, and we discuss the RPDFs for three specific distributions. One choice is a (one-dimensional) Jüttner distribution, which is the relativistic thermal distribution $f(u) \propto \exp(-\rho\gamma)$, with $\rho = m/T$, where T is the temperature in energy units. A second class of distributions are bell-like, and involve generalizing a waterbag distribution ($f(u) =$ constant for $-u_m < u < u_m$ and $f(u) = 0$ otherwise), the RPDF for which was introduced by Arons and Barnard (1986). As pointed out by Gedalin et al. (1998), the RPDF for this distribution is singular at the parallel phase velocities ($z = \omega/k_\parallel = \pm v_m$) at which the distribution function is discontinuous, and it cannot be used to discuss Landau damping. Gedalin et al. (1998) introduced the class of bell-like distribution functions ($f_n(u) \propto (u^2 - u_m^2)^n$) in which the discontinuous cutoff in the waterbag distribution is replaced by a continuous cutoff, with a discontinuity only in its nth derivative. This class of distributions has the advantage that the RPDF can be evaluated explicitly in terms of polynomials and logarithmic functions of z. In our numerical calculations, we choose $n = 3$. The third class of distribution is the Gaussian function $f(u) \propto \exp(-u^2/2u_m^2)$ chosen by Lominadze and Mikhailovskii (1979). (Suvorov and Chugunov (1975) considered a distribution $f(u) \propto (1+u^2)^{-3/2}$, but they evaluated the response tensor explicitly only in the case of perpendicular propagation, when a RPDF is unnecessary, and their claim of the non-existence of subluminal Langmuir waves in the case of parallel propagation is based on an inadequate treatment of the dispersion (Lominadze and Mikhailovskii 1979); we do not discuss this choice of distribution function here.) We find that in the extremely relativistic limit, the important features in the RPDF are not particularly sensitive to the choice of these three forms for $f(u)$.

In Sec 2, we write down the components of the relevant dielectric tensor, define the RPDF and discuss it for our three choices of distribution function.

https://doi.org/10.1017/S0022377899007795 Published online by Cambridge University Press

In Sec. 3, we show how the RPDF changes as the plasma becomes increasingly intrinsically relativistic. In Sec. 4, we use the RPDF to discuss the wave properties, concentrating on parallel and nearly parallel waves. In Sec. 5 we discuss the significance of our results.

2. Relativistic plasma dispersion function

We follow Gedalin et al. (1998) in writing down the components of the dielectric tensor in the rest frame of a pair plasma. The plasma is assumed to be one-dimensional, with identical distributions of electrons and positrons. The wave frequency is assumed to be small compared with the cyclotron frequency of the particles, $\omega \ll \Omega_e/\langle\gamma\rangle$, where $\Omega_c = eB/m$ is the (nonrelativistic) cyclotron frequency. The number density n and the mean Lorentz factor $\langle\gamma\rangle$ are used to define the plasma frequency and the Alfvén speed,

$$\omega_p = \left(\frac{e^2 n}{\varepsilon_0 m}\right)^{1/2}, \qquad v_A = \langle\gamma\rangle^{-1/2}\frac{\Omega_e}{\omega_p}. \tag{2.1a,b}$$

Another parameter that appears is the mean square speed Δv^2, defined by writing

$$\langle\gamma v_\parallel^2\rangle = \langle\gamma\rangle\,\Delta v^2, \qquad \Delta v^2 = 1 - \frac{\langle\gamma^{-1}\rangle}{\langle\gamma\rangle}. \tag{2.2a,b}$$

The distinguishing feature of an intrinsically relativistic plasma is that one has $\Delta v^2 \sim 1$, rather than $\Delta v^2 \ll 1$ in a nonrelativistic plasma.

2.1. The dielectric tensor

The dielectric tensor $K_{ij}(\omega, \mathbf{k})$ has the following form in a coordinate system in which the magnetic field is along the 3-axis, and $\mathbf{k}$ is in the 1–3 plane at an angle θ to the magnetic field (GMG):

$$K_{11} = K_{22} = a + \frac{1-b}{z^2}, \tag{2.3a}$$

$$K_{13} = K_{31} = -\frac{1-b}{z^2}\tan\theta, \tag{2.3b}$$

$$K_{33} = 1 - \frac{\omega_p^2}{\omega^2} z^2 W(z) + \frac{1-b}{z^2}\tan^2\theta, \tag{2.3c}$$

$$a = 1 + \frac{1}{v_A^2}, \qquad b = 1 - \frac{\Delta v^2}{v_A^2}, \tag{2.3d,e}$$

with $z = \omega/k_\parallel$. The gyrotropic terms $K_{12} = -K_{21}$ and $K_{23} = -K_{32}$ are zero for identical electron and positron distributions. Only terms up to order $1/\Omega_e^2$ are retained in an expansion in $1/\Omega_e$, and all effects associated with the cyclotron resonance are ignored (cf. Mikhailovskii et al. 1982).

The gyrotropic terms, appearing when the two species move relative to each other, are of the order of $(\omega_p^2/\Omega_e w)\,\delta n/n$ or $(\omega_p^2/\Omega\omega)\,J/nc$ (see Gedalin et al. 1998), where δn is the difference between the electron and positron number densities, and J is the current density produced by this shift of the distribution

https://doi.org/10.1017/S0022377899007795 Published online by Cambridge University Press

functions. The ratios are at most $\delta n/n \sim J/nc \sim 1/M$, where M is the multiplicity factor, and so are small for large M. Moreover, these terms appear in the dispersion equation only quadratically, so that their contribution is a factor $1/M^2$ smaller than the contribution due to the nongyrotropic terms. These terms need to be taken into account for extremely low-frequency waves, which are not discussed here. Their main role for the waves of interest here is to change the wave polarization from linear to elliptical (circular for parallel propagation). Their effect, for $M \gg 1$, on the dispersion characteristics of the waves in the frequency range under consideration is small.

2.2. The relativistic plasma dispersion function (RPDF)

The RPDF that appears in (2.3) is denoted by $W(z)$, and is defined by

$$W(z) = \int_{-\infty}^{\infty} \frac{du}{v-z}\frac{df(u)}{du} = \int_{-1}^{1} \frac{dv}{v-z}\frac{df(u)}{dv}, \tag{2.4a}$$

$$\int_{-\infty}^{\infty} du f(u) = \int_{-1}^{1} dv\, \gamma^3 f(u) = 1. \tag{2.4b}$$

Below, we consider general properties of the RPDF and evaluate it for three specific forms of $f(u)$.

2.3. General properties of RPDF

Since the RPDF plays a crucial role in the determination of the wave features, we consider here its general properties independent of the choice of the distribution function.

For $z > 1$, the RPDF (2.4) has no singularities, and partial integration gives

$$W(z) = \int_{-\infty}^{\infty} \frac{f(u)\,du}{\gamma^3 (z-v)^2} > 0. \tag{2.5}$$

In the limit $z \to \infty$, one has $z^2 W(z) \to \langle \gamma^{-3} \rangle$. At $z = 1$, one has $W(1) = \langle \gamma \rangle - \langle \gamma^{-1} \rangle$. In the limit $z = 0$, one has

$$W(0) = \mathscr{P} \int \frac{du}{v}\frac{df}{du}. \tag{2.6}$$

If the distribution is symmetric ($f(-u) = f(u)$) and monotonically decreasing ($u\,df/du < 0$), (2.6) implies $W(0) < 0$. These properties imply that there is a zero of $W(z)$ in the range $0 < z < \infty$. At least for the monotonic distribution functions considered here, there is only one such zero, and we denote it by $z = z_0$, so that we have $\mathrm{Re}[W(z_0)] = 0$.

Physically, the limit $\omega \to 0$ at nonzero k ($z \to 0$) gives $K_{33} = 1 + 1/k^2\lambda_D^2$, and so $W(0)$ determines the Debye length λ_D by $1/\lambda_D^2 = -\omega_p^2 W(0)$. The limit $k \to 0$ ($z \to \infty$) gives the cutoff frequency ω_c for Langmuir waves. In a nonrelativistic plasma, one has $z^2 W(z) \to 1$ for $z \to \infty$, implying that $\omega_c = \omega_p$. In a relativistic plasma, one has $z^2 W(z) \to \langle \gamma^{-3} \rangle$ for $z \to \infty$, and hence

$$\omega_c^2 = \omega_p^2 \langle \gamma^{-3} \rangle, \tag{2.7}$$

with $\langle \gamma^{-3} \rangle \sim 1/\langle \gamma \rangle$ in an intrinsically extremely relativistic plasma.

We analyse in detail the RPDF for the one-dimensional Jüttner distribution for bell-like distributions, and for a Gaussian distribution.

https://doi.org/10.1017/S0022377899007795 Published online by Cambridge University Press

2.4. One-dimensional Jüttner distribution

A one-dimensional Jüttner (relativistic thermal) distribution is

$$f(u) = \frac{1}{2K_1(\rho)} e^{-\rho\gamma}, \tag{2.8}$$

where $\rho = m/T$ is the inverse temperature in units of the rest mass and $K_\nu(\rho)$ is a Macdonald function (a modified Bessel function). In this case, we have

$$\langle\gamma\rangle = \frac{K_0(\rho)+K_2(\rho)}{2K_1(\rho)} \approx \frac{1}{\rho}, \tag{2.9}$$

where the approximate value applies in the extremely relativistic limit $\rho \ll 1$.

Various RPDFs have been defined for an isotropic Jüttner distribution in connection with waves in isotropic relativistic plasmas (see e.g. Trubnikov 1958; Silin 1960; Kurşunoğlu 1961; Imre 1962; Prentice 1967; Hakim and Mangeney 1971; Polyakov 1983; Magneville 1990). Our choice is related simply to the RPDF defined by Godfrey et al. (1975b),

$$T(z,\rho) = \int_{-1}^{1} dv\, \frac{e^{-\rho\gamma}}{v-z}, \tag{2.10}$$

and used by them to treat both the one-dimensional and isotropic cases. On inserting (2.8) in (2.4), one has

$$z^2 W(z) = \frac{z^2 T'(z,\rho)}{2K_1(\rho)}. \tag{2.11}$$

The imaginary part of this RPDF is

$$\frac{z^2\,\mathrm{Im}[T'(z,\rho)]}{2K_1(\rho)} = \frac{\pi\rho\gamma_0^3 z^3}{2K_1(\rho)} \exp(-\rho\gamma_0), \tag{2.12}$$

implying that Landau damping is weak but not strictly zero for $1/\rho \ll \gamma_0 < \infty$, and strictly zero for superluminal waves ($z > 1$).

2.5. The RPDF for $f_n(u)$

A bell-type distribution is of the form

$$f_n(u) = A_n(u_m)\,(u_m^2 - u^2)^n\, H(u_m^2 - u^2), \tag{2.13a}$$

$$A_n^{-1}(u_m) = \int_{-u_m}^{u_m} du\,(u_m^2 - u^2)^n, \tag{2.13b}$$

where $H(x)$ is the step function. The case $n = 0$ corresponds to a waterbag distribution, and $n = 1$ and $n = 2$ to the hard-bell and soft-bell distributions (Gedalin et al. 1998) respectively.

The RPDF, $z^2 W(z) = z^2 W_n(v_m, z)$, for this class of distribution functions is

$$z^2 W_n(v_m, z) = \frac{-2n\Gamma(n+\frac{3}{2})\,(1-v_m^2)^{3/2} z^2}{\pi^{1/2}\Gamma(n+1) v_m^{2n+1}} \int_{-v_m}^{v_m} dv\, \frac{v(v_n^2 - v^2)^{n-1}}{(1-v^2)^{n+1}(v-z)}. \tag{2.14}$$

The integral may be performed analytically (see the Appendix). The explicit

https://doi.org/10.1017/S0022377899007795 Published online by Cambridge University Press

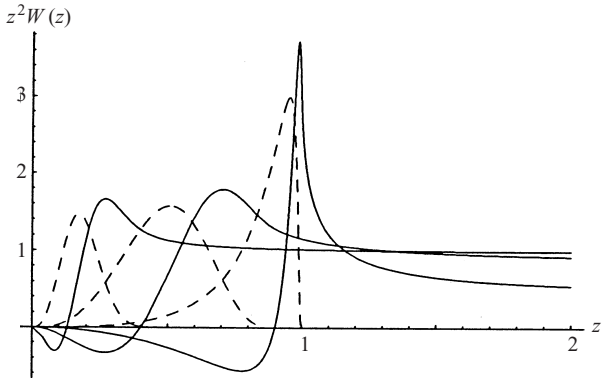


Figure 1. The RPDF $z^2W(z)$ is plotted as a function of phase speed z for three Jüttner distributions, with the solid curves showing the real parts and the dashed curves the imaginary parts: $\rho = 100$ (leftmost curves), $\rho = 10$ (centremost curves), $\rho = 1$ (rightmost curves).

forms were written down by Gedalin et al. (1998) for $n = 1, 2$, and the explicit form for $n = 3$ is written down in the Appendix. The Landau prescription implies the imaginary part

$$z^2\,\mathrm{Im}[W_n(v_m, z)] = \pi \frac{2n\Gamma(n+\frac{3}{2})\,(1-v_m^2)^{3/2}}{\pi^{1/2}\Gamma(n+1)v_m^{2n+1}} \frac{z^3(v_n^2-z^2)^{n-1}}{(1-z^2)^{n+1}} H(v_n^2-z^2). \quad (2.15)$$

2.6. The Gaussian distribution

The Gaussian distribution, chosen by Laminadze and Mikhailovskii (1979), is

$$f(u) = \frac{1}{\pi^{1/2}u_m} \exp\left(-\frac{u^2}{2u_m^2}\right). \quad (2.6)$$

The real part of the RPDF,

$$z^2W(z) = -\frac{1}{\pi^{1/2}u_m^3} \int_{-1}^{1} dv\, \frac{v}{(1-v^2)^{3/2}(v-z)} \exp\left[-\frac{v^2}{2u_m^2(1-v^2)}\right], \quad (2.17)$$

needs to be evaluated numerically. The imaginary part is

$$z^2\,\mathrm{Im}[W(z)] = \left(\frac{\pi}{2}\right)^{1/2} \frac{z^3\gamma_0^4}{u_m^3} \exp\left(-\frac{z^2\gamma_0^2}{2u_m^2}\right). \quad (2.18)$$

3. Properties of the RPDF: numerical illustration

In this section, we discuss the properties of the RPDF, emphasizing numerical results. The RPDF appears only in the component K_{33} in (2.3), and this describes the parallel, longitudinal response of the plasma for $\theta = 0$, when we have $K_{33} = 1-(\omega_p^2/\omega^2)\,z^2W(z)$.

3.1. Transition from nonrelativistic to relativistic temperatures

The RPDF in nonrelativistic, and mildly relativistic thermal plasmas is plotted in Fig. 1. The values chosen, $\rho = 100$, 10 and 1, correspond to $T = 5.1$ keV, 51 keV and 511 keV respectively.

https://doi.org/10.1017/S0022377899007795 Published online by Cambridge University Press

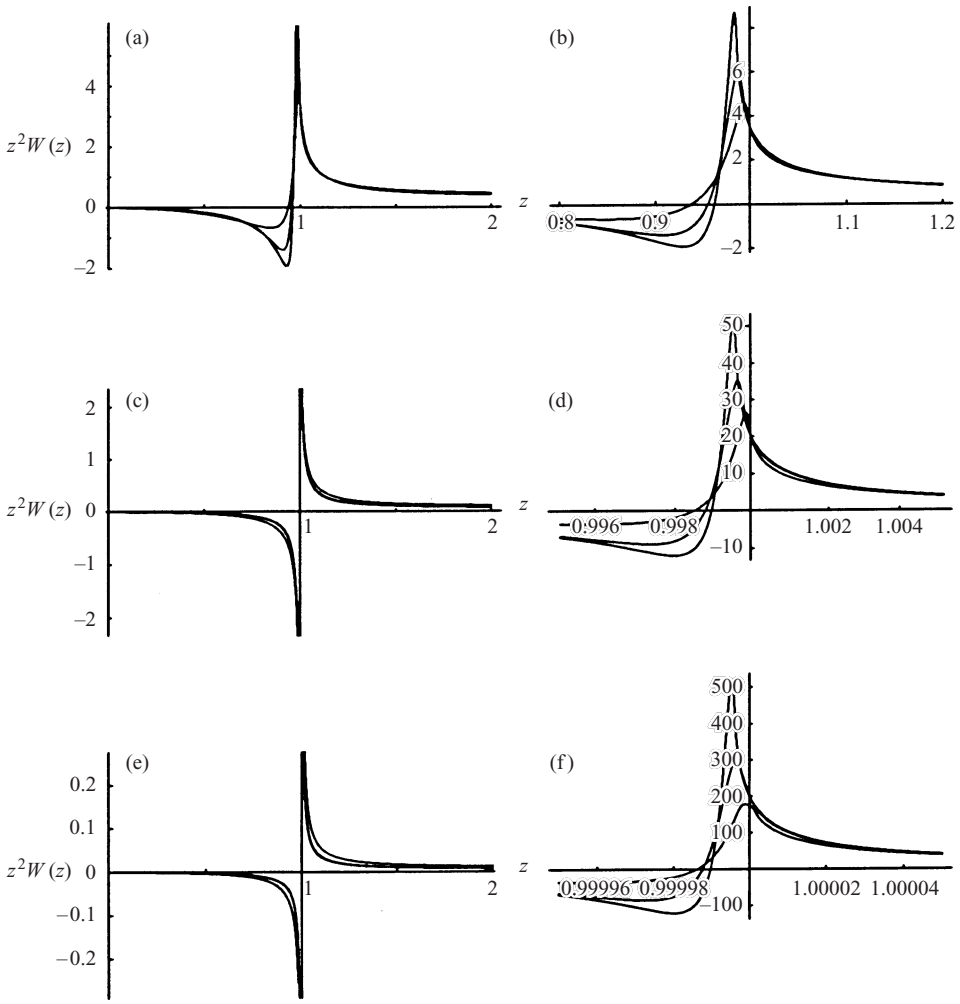


Figure 2. (a) The RPDFs for the three distribution functions are shown for the same value of $\langle\gamma\rangle = 2$. (b) The region near the peaks in the RPDF is shown on a different scale. (c) and (d) are as for (a) and (b), but for $\langle\gamma\rangle = 10$. (e) and (f) are as for (a) and (b), but for $\langle\gamma\rangle = 100$.

In the nonrelativistic limit, the RPDF reduces to the familiar nonrelativistic plasma dispersion function (see e.g. Melrose 1986, p. 23). As z increases, $z^2W(z)$ decreases from 0 at $z = 0$ to a maximum negative value; it then increases, crosses zero at $z = z_0$, rises to a peak, and then decreases monotonically to unity ($[z^2W(z)]_\infty = 1$) for $z \to \infty$. Let us denote by $z = z_{\rm peak}$ the value at which the peak occurs ($z^2_{\rm peak}\, W(z_{\rm peak}) = [z^2W(z)]_{\rm peak}$). As $\langle\gamma\rangle - 1$ increases through mildly relativistic values, $[z^2W(z)]_{\rm peak}$ increases and its location moves closer to $z = 1$. Using the partially integrated form (2.5) to evaluate the RPDF where it crosses the light line $z = 1$, its value there is $\langle\gamma\rangle - \langle\gamma^{-1}\rangle$; this value increases as $\langle\gamma\rangle$ increases. The peak value $[z^2W(z)]_{\rm peak}$ is significantly higher than the value $W(1)$ at the light line, but for large $\langle\gamma\rangle$ they are of the same order in an expansion in $1/\langle\gamma\rangle$. The asymptotic value, which is $[z^2W(z)]_\infty = \langle\gamma^{-3}\rangle$ according to (2.7), decreases to significantly less than unity as $\langle\gamma\rangle$ increases. Thus the most

https://doi.org/10.1017/S0022377899007795 Published online by Cambridge University Press

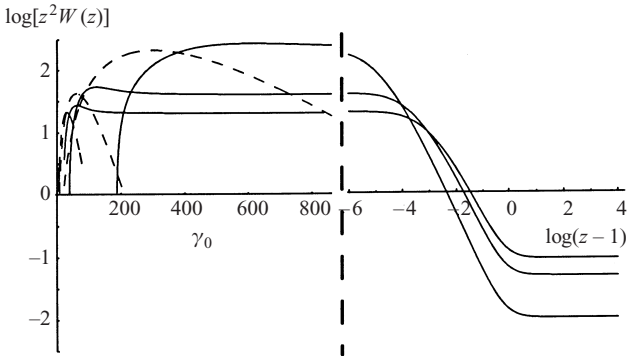


Figure 3. The RPDF for a Jüttner distribution is plotted for three values $\rho = 0.1$, 0.05 and 0.01 corresponding to an extremely relativistic plasma. In order to show the extremely large peak just below $z = 1$, the logarithm of $z^2W(z)$ is plotted as a function of $\gamma_0 = 1/(1-z^2)^{1/2}$ for $z < 1$ and as a function of $\log(z-1)$ for $z > 1$. As in Fig. 1, the solid curves show the real parts and the dashed curves the imaginary parts.

obvious features of the RPDF in a relativistic plasma are the very large peak ($> \langle\gamma\rangle$) just below $z = 1$ ($z_{\rm peak} - 1 \sim 1/\langle\gamma\rangle$), and the very small ($= \langle\gamma^{-3}\rangle \sim 1/\langle\gamma\rangle$) asymptotic value.

3.2. Dependence on the choice of distribution function

In Fig. 2, we compare the RPDFs for our three choices of distribution functions for fixed values of $\langle\gamma\rangle = 2$, 10 and 100. The form of the RPDF for $z \geqslant 1$ is severely constrained by the values at $z = 1$ and $z = \infty$, which are $\langle\gamma\rangle - \langle\gamma^{-1}\rangle$ and $\langle\gamma^{-3}\rangle$ respectively. The differences in the RPDFs for different choices of $f(u)$ in the range $z > 1$ are effectively due to the small differences between the values of $\langle\gamma^{-1}\rangle$ and $\langle\gamma^{-3}\rangle$ at fixed $\langle\gamma\rangle$ for the three distribution functions.

The main differences in the RPDFs for the different choices of $f(u)$ are in the peak value, the location of the peak and the width of the peak. The Jüttner distribution gives the lowest peak value, the broadest peak and the peak value closest to $z = 1$ for a given value of $\langle\gamma\rangle$. The highest peak is for $f_3(u)$ and the intermediate peak for the Gaussian distribution. These differences are relatively minor when one takes into account the very strong dependence on the value of $\langle\gamma\rangle$.

As the plasma becomes relativistic, it is not possible to display the functional form adequately on a single plot of $z^2W(z)$ versus z, and two separate plots are shown for each of the cases in Fig. 2. Even this format becomes inadequate for extremely relativistic values $\langle\gamma\rangle \gg 1$. In Fig. 3, the logarithm of the RPDF (for $z > z_0$ where the function is positive) for a Jüttner distribution is plotted for three extremely relativistic values, $\langle\gamma\rangle = 10$, 20 and 100, as a function of $\gamma_0 = (1-z^2)^{-1/2}$ for $z < 1$ and as a function of the logarithm of $z-1$ for $z > 1$. The values at the peak, at $z = 1$ and for $z \to \infty$ are clearly displayed on such a plot.

4. Parallel and nearly parallel waves

The RPDF introduction in Sec. 2 is used in this section to derive the properties of waves for parallel propagation ($\theta = 0$) in the extremely relativistic limit $\langle\gamma\rangle \gg 1$. As mentioned in Sec. 1, in the extensive literature on wave dispersion,

https://doi.org/10.1017/S0022377899007795 Published online by Cambridge University Press

most authors have avoided using a RPDF by making various simplifying assumptions, and, in this section and the next, we concentrate on the features for which use of a RPDF is essential.

4.1. The wave equation

The wave equation may be written (see e.g. Volokitin et al. 1985; Gedalin et al. 1998)

$$\Lambda_{ij}\, e_j = 0, \qquad \Lambda_{ij} = n_i\, n_j - n^2 \delta_{ij} + K_{ij}, \tag{4.1a,b}$$

where $\mathbf{n} = \mathbf{k}/\omega$ has components $n_1 = \tan\theta/z$, $n_2 = 0$, $n_3 = 1/z$, and where the polarization vector $\mathbf{e}$ is a unimodular vector along the electric field in the waves. On inserting the form (2.3) for K_{ij}, the nonzero components of Λ_{ij} are

$$\Lambda_{11} = a - \frac{b}{z^2}, \qquad \Lambda_{22} = a - \frac{b - \sin^2\theta}{z^2}, \tag{4.2a,b}$$

$$\Lambda_{13} = \Lambda_{31} = \frac{b}{z^2}\tan\theta, \tag{4.2c}$$

$$\Lambda_{33} = 1 - \frac{\omega_p^2}{\omega^2} z^2 W(z) - \frac{b}{z^2}\tan^2\theta. \tag{4.2d}$$

The dispersion equation is

$$\begin{vmatrix} \Lambda_{11} & 0 & \Lambda_{13} \\ 0 & \Lambda_{22} & 0 \\ \Lambda_{13} & 0 & \Lambda_{33} \end{vmatrix} = 0, \tag{4.3}$$

which factorizes into two equations,

$$\Lambda_{22} = 0, \tag{4.4}$$

$$\Lambda_{11}\Lambda_{33} - \Lambda_{13}^2 = 0. \tag{4.5}$$

Equation (4.4) gives the dispersion relation for the magnetoacoustic (or X or t) mode. Equation (4.5) gives the dispersion equation for the L-O mode and the Alfvén mode. The polarization vector for the magnetoacoustic mode is along the 2-axis, and the polarization vector for the other two modes is in the 1–3 plane, with

$$\frac{e_1}{e_3} = -\frac{\Lambda_{33}}{\Lambda_{13}} = -\frac{\Lambda_{13}}{\Lambda_{11}}, \tag{4.6}$$

which are to be evaluated at the appropriate solution of the dispersion equation (4.5). Here we are concerned only with the wave modes that depend on the RPDF, and these are the solution of (4.5). The magnetoacoustic mode does not involve the RPDF, and is not discussed further here (see Gedalin et al. 1998).

4.2. Parallel propagation

The dispersion relation for parallel Langmuir waves follows from (4.5) for $\theta = 0$. One then has $\Lambda_{13} = 0$, and the equation factorizes into $\Lambda_{11} = 0$, which defines the parallel Alfvén mode, and $\Lambda_{33} = 0$, which defines the parallel Langmuir mode. The latter gives the dispersion relation

$$\omega^2 = \omega_p^2\, z^2 W(z). \tag{4.7}$$

https://doi.org/10.1017/S0022377899007795 Published online by Cambridge University Press

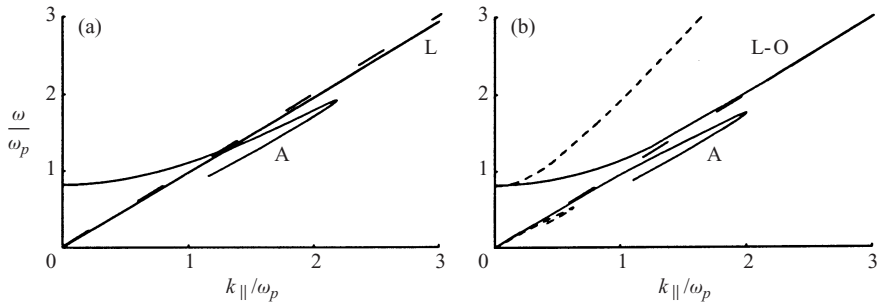


Figure 4. Dispersion curves are shown for $f_3(u)$ with $v_m = 0.9$ and $z_A = 0.95$. The dashed diagonal line is the light line. (a) For parallel propagation, the solid straight line just to the right of the light line is the dispersion curve for the parallel Alfvén wave, and the other curve is for the Langmuir wave, which has a maximum frequency, with a heavily damped branch or reverse dispersion to the right of the main dispersion curve. (b) As for (a), but for oblique propagation, with $\theta = 0.1$ for the solid curves and $\theta = 1$ for the dashed curves; the dispersion curves reconnect, with the upper branch being the L-O mode and the lower branch being the oblique Alfvén mode.

The wave damping rate is given by

$$\mathrm{Im}\,\omega = \frac{\omega_p^2}{\omega^2} z^2\,\mathrm{Im}[W(z)], \tag{4.8}$$

and is nonzero only for $z < v_m$ for bell-type distributions and for $z < 1$ for the Jüttner and Gaussian distributions.

Equation (4.7) has solutions only for $z > z_0$. When $z \to z_0$ from above, the Langmuir wave frequency $\omega \to 0$ and Im W remains finite, which means that the 'wave' is strongly damped, and in fact does not exist. We assume that the whole part of the branch corresponding to $z_0 < z < z_{\mathrm{peak}}$ is strongly damped, and we ignore it in the following discussion.

The two other dispersion relations are $\Lambda_{11} = \Lambda_{22} = 0$. These describe two degenerate electromagnetic waves with dispersion relation

$$z = z_A, \qquad z_A = \left(\frac{b}{a}\right)^{1/2} = \left(\frac{v_A^2 - \Delta v^2}{1 + v_A^2}\right)^{1/2}, \tag{4.9a,b}$$

where the Alfvén speed v_A is defined by (2.1) and Δv^2 is defined by (2.2). This double solution corresponds to the magnetoacoustic and Alfvén waves in the degenerate case of parallel propagation, where both modes are undamped. The parallel electromagnetic and Langmuir modes are independent for $z < z_0$, they intersect in the region of strong damping for the Langmuir mode for $z_0 < z_A \lesssim z_{\mathrm{peak}}$, and they intersect in the region of weak damping for $z_0 \gtrsim z_{\mathrm{peak}}$.

4.3. Parallel propagation: numerical results

The dispersion relations are illustrated on an (ω, k) plot in Fig. 4(a) for a mildly relativistic plasma. As $\langle\gamma\rangle$ increases, the cutoff frequency of the Langmuir wave decreases and the maximum frequency increases. In the extremely relativistic limit, the two are widely separated, with the dispersion curve being close to the light line, on the superluminal side of it, over a range $\omega_p/\langle\gamma\rangle^{1/2} \lesssim \omega \lesssim \omega_p\langle\gamma\rangle^{1/2}$.

https://doi.org/10.1017/S0022377899007795 Published online by Cambridge University Press

The dispersion curves in Fig. 4 are shown to extend from $z = \infty$ to the peak in $z^2W(z)$ at $z = z_{\rm peak}$ and then through the region of inverse dispersion in the range $z_0 < z < z_{\rm peak}$. However, Landau damping is neglected in the derivation of these curves, and this neglect needs to be justified. Both the real and imaginary parts of $z^2W(z)$ are plotted in Figs 1 and 3. The imaginary part is small compared with the real part at phase speeds $z \gg z_{\rm peak}$ above the peak in the real part, and is large compared with the real part for $z \ll z_{\rm peak}$. This result is insensitive to the functional form of the distribution and to whether it is nonrelativistic, mildly relativistic or extremely relativistic. As remarked above, Landau damping is strong for $z \lesssim z_{\rm peak}$, and the region of inverse dispersion is neglected here because the assumption of weak damping is invalid.

4.4. Oblique propagation: general case

The general dispersion equation for oblique propagation can be written in the form

$$\frac{\omega^2}{\omega_p^2} = \frac{z^2W(z)\,(z^2 - z_A^2)}{z^2 - z_A^2 - b\tan^2\theta}, \tag{4.10}$$

with $z_A^2 = b/a$; cf. (4.9). It is convenient to write

$$z_B^2 = z_A^2 + b\tan^2\theta \approx \frac{1}{\cos^2\theta}\left(1 - \frac{\Delta v^2 + \cos^2\theta}{v_A^2}\right), \tag{4.11}$$

where the approximation involves ignoring higher-order terms in an expansion in $1/v_A^2$. The limit of the infinite magnetic field, which corresponds to $z_A \to 1$ and $z_B \to 1/\cos\theta$, was discussed by Gedalin et al. (1998).

Equation (4.10) has a physically relevant solution only if the right-hand side is positive. Assuming $z > 0$, the sign is determined by the signs of $W(z)$, which is positive for $z > 0$, and of $z - z_A$ and $z - z_B$. The inequality $z_A < z_B$ implies that there are only three possible cases: $z_0 < z_A, z_A < z_0 < z_B$ and $z > z_B$. A solution is possible for $z_A < z < z_0, z_B$, but Landau damping is strong for $z < z_0$, and we ignore this possibility on the grounds that it does not correspond to weakly damped waves. There are then only two possibilities for weakly damped waves: $z_0 < z < z_A$ and $z_0, z_B < z$. We refer to these two branches as the Alfvén mode and the L-O mode respectively.

The L-O mode extends to $\omega \to \infty$, and the Alfvén-mode frequency is limited to frequencies below some maximum value. It was shown in Gedalin et al. (1998) that in the strong-field limit ($z_A \to 1$), the Alfvén mode is strongly damped for $z < z_{\rm peak}$, and that the maximum frequency of the Alfvén mode is at $z = z_{\rm peak}$. The damping is due to the imaginary part of W, and is insensitive to the corrections related to finiteness of the external magnetic field. The L-O mode is superluminal except for $\theta \lesssim 1/v_A$, that is, except for nearly parallel propagation. The case of substantially oblique propagation does not differ much from the strong-field limit discussed by Gedalin et al. (1998). The case of nearly parallel propagation is considered in detail below.

4.5. Slightly oblique propagation

For $z_A \gtrsim z_{\rm peak}$, the Alfvén and Langmuir modes intersect for parallel propagation, and for $\theta \neq 0$ they reconnect to form the (oblique) Alfvén and L-O modes, as pointed out by Hardee and Rose (1976) in the case where there is

https://doi.org/10.1017/S0022377899007795 Published online by Cambridge University Press

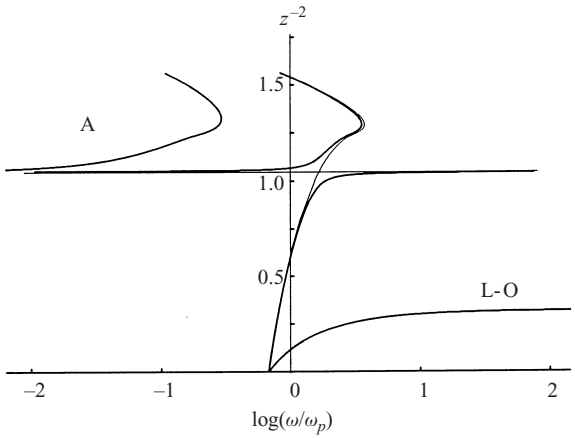


Figure 5. The dispersion curves shown in Fig. 4 are plotted in terms of $1/z^2$ as a function of ω/ω_p. The results for $\theta = 0$ are shown by the thin curves, the inner solid curves are for $\theta = 0.1$ and the outer solid curves are for $\theta = 1$.

no spread in particle energies. In terms of the RPDF, the intersection point for $\theta = 0$ defines a crossover frequency $\omega_{\rm co}$:

$$\omega_{\rm co} = \omega_p[z_A^2\, W(z_A)]^{1/2}, \tag{4.12}$$

with the corresponding wavenumber $= \omega_{\rm co}/z$. As illustrated in Fig. 4(b), for small θ, the two modes deviate from each other with increasing θ. The higher-frequency reconnected mode is the L-O mode. For small θ, the L-O mode differs little from the parallel Langmuir mode for $\omega \lesssim \omega_{\rm co}$, and it becomes the ordinary mode (O mode) for $\omega \lesssim \omega_{\rm co}$. Our discussion is restricted to frequencies below the relativistic gyrofrequency, so that our results for the properties of the O mode and X mode are valid only in this limit.

The results in Fig. 4 are for a mildly relativistic plasma, and, although the results in the extremely relativistic case are an obvious extension of them, they cannot be shown easily in the format of Fig. 4. In Fig. 5, we replot the curves from Fig. 4 in a format that does facilitate extension to the extremely relativistic limit. This involves plotting $1/z^2$, which is the square of the refractive index for parallel propagation, as a function of ω/ω_p. An example of the extremely relativistic limit is shown in this format in Fig. 6. As $\langle\gamma\rangle$ increases, the reconnection and significant separation of the modes in ω/ω_p is restricted to narrower and narrower ranges of $z \approx z_A$ and $\theta \approx 0$.

For $\omega \gtrsim \omega_{\rm co}$, the L-O mode is indistinguishable from the parallel Alfvén mode for sufficiently small θ, and it deviates to higher frequencies (or higher z) as θ increases, lying entirely in the superluminal range for θ greater than a minimum value. Thus the L-O mode extends from the cutoff in the Langmuir mode to arbitrarily high frequencies. (Recall, however, that the discussion here is specifically only for frequencies below the cyclotron frequency of the particles.) We refer to the lower-frequency reconnected mode as the oblique Alfvén mode or simply the Alfvén mode. It is indistinguishable from the parallel Alfvén mode for sufficiently small θ, and it deviates to lower frequencies (or lower z) as θ increases. The maximum frequency, originally identified as in the parallel Langmuir mode, is actually in the reconnected Alfvén mode. The existence of a maximum frequency for the Alfvén mode was indicated schematically by

https://doi.org/10.1017/S0022377899007795 Published online by Cambridge University Press

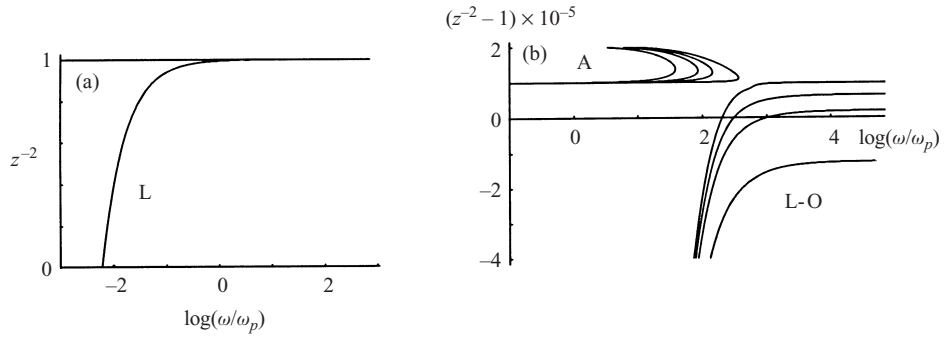


Figure 6. As Fig. 5, but for $\langle\gamma\rangle = 100$, $b = 0.9$, $1-z_A = 10^{-5}$, and with $1/z^2$ plotted as a function of $\log(\omega/\omega_p)$. (a) The Langmuir mode is the rising curve, and the Alfvén mode is indistinguishable from a horizontal line at $z = 1$. (b) On a different scale for $\theta = 0.5\times10^{-3}$ (innermost curves), 1×10^{-3}, 2×10^{-3}, 5×10^{-3} (outermost curves).

Volokitin et al. (1985), and its existence was discussed further by Gedalin et al. (1998). A new point noted here is that a physically important reconnection between the Alfvén and L-O modes occurs if the phase speed z_A of the parallel Alfvén waves exceeds the minimum phase speed of the parallel Langmuir waves, corresponding effectively to the maximum frequency of the Langmuir waves. For $z_A \lesssim z_{\rm peak}$, the phase speed of the Alfvén waves is in the region of inverse dispersion of the Langmuir waves and of strong Landau damping. Although parallel Alfvén waves are undamped, because their electric vector is strictly orthogonal to **B**, oblique Alfvén waves are weakly damped only for a small range of $\theta \approx 0$, and become more strongly damped with increasing θ owing to the increasing value of E_z/E_x. No intersection of the dispersion curves occurs for $z_A < z_0$.

5. Discussion and conclusions

The relativistic plasma dispersion function (RPDF) appropriate for an intrinsically extremely relativistic, strongly magnetized, one-dimensional pair plasma is found to have the following properties in the rest frame of the plasma.

(*a*) The RPDF $z^2W(z)$ has an extremely high peak ($=\langle\gamma\rangle-\langle\gamma^{-1}\rangle \approx \langle\gamma\rangle$), at a phase speed $z_{\rm peak}$ close to unity ($1-z_{\rm peak} \sim 1/\langle\gamma\rangle$).

(*b*) The height, location and width of the peak depend weakly on the form of $f(u)$ at fixed $\langle\gamma\rangle$, being lowest nearest $z = 1$ and broadest for a Jüttner distribution.

(*c*) The asymptotic value for the RPDF is extremely small ($=\langle\gamma^{-3}\rangle \sim 1/\langle\gamma\rangle$ for $z\to\infty$).

(*d*) The shape of the RPDF is not sensitive to the choice of distribution function for $z \gtrsim 1$.

(*e*) The imaginary part is larger than the real part only for $z \lesssim z_{\rm peak}$, as in a nonrelativistic plasma.

These properties have implications for the properties of waves in such plasmas. We identify two features of the wave properties that depend explicitly on the RPDF. First, the parallel Langmuir mode has a maximum frequency,

https://doi.org/10.1017/S0022377899007795 Published online by Cambridge University Press

determined by the peak at $z = z_{\rm peak}$ in the RPDF. There is a region of inverse dispersion at slightly lower phase speeds, but this is in the range where Landau damping is strong. Secondly, for slightly oblique waves, the reconnection between the Langmuir mode and the Alfvén (Hardee and Rose 1976) mode effectively occurs only for $z_A > z_{\rm peak}$, cf. (4.9), and when this condition is satisfied, the reconnection occurs at the crossover frequency $\omega_{\rm co}$ given by (4.12). The peak value then occurs in the (reconnected) Alfvén mode and determines its maximum frequency. The lower-frequency branch of the reconnected mode is the oblique Alfvén mode, and the maximum frequency, which is in the Langmuir mode for $\theta = 0$, is in the oblique Alfvén mode for $\theta \neq 0$. The existence of a maximum frequency in the Alfvén mode was indicated schematically by Volokitin et al. (1985), and discussed further by Gedalin et al. (1998). The higher-frequency branch of the reconnected mode extends from the cutoff frequency for the Langmuir mode to arbitrarily high frequencies, where it becomes the O-mode.

We propose to discuss the astrophysical implications of these results in detail elsewhere. In brief, in order for a beam instability to generate waves, the beam speed v_b must exceed the phase speed z of the waves. In a plasma with the properties considered here, this requirement has the following implications. For parallel Langmuir waves, the requirement is satisfied only for waves with frequency $\omega \sim \omega_p \langle\gamma\rangle^{1/2}$, which is a factor of order $\langle\gamma\rangle$ higher than the cutoff frequency for Langmuir waves. For oblique waves, the requirement $v_b > z$ has different implications for $v_b > z_A$ and $v_b < z_A$, where z_A is the phase speed of parallel Alfvén waves, cf. (4.9). For $v_b > z_A$, a beam instability is possible in both the L-O and oblique Alfvén modes, but only in a restricted range of angles for the L-O mode where the waves have $z < v_b$. For $v_b < z_A$, a beam instability is not possible in the L-O mode, and is possible in the oblique Alfvén mode, but only for angles greater than a minimum value where the waves have $z < v_b$. These properties prove to be extremely restrictive, to the extent that this favoured mechanism may be untenable.

Two assumptions made in the present investigation need to be relaxed in a more general discussion. First, the discussion here is restricted to frequencies below the relativistic gyrofrequency, and relaxing this assumption is important in order to discuss the escape of radiation from a pulsar plasma (Mikhailovskii et al. 1982). Secondly, the gyrotropic terms ($K_{12} = -K_{21}, K_{23} = -K_{32}$) are neglected here, and they are nonzero in a pulsar plasma owing to nonzero charge and current (respectively) densities; relaxation of this assumption is important for any discussion of the circular polarization of the natural modes, which is determined by these gyrotropic terms.

Acknowledgement

We thank Iver Cairns for helpful comments on the manuscript.

Appendix. Analytical evaluation of $W_n(v_m, z)$

Calculation of the RPDF (2.14) requires evaluation of the integrals

$$A_n = \mathscr{P} \int_{-v_m}^{v_m} dv \, \frac{v(v_m^2 - v^2)^{n-1}}{(1-v^2)^{n+1}(v-z)}. \tag{A 1}$$

https://doi.org/10.1017/S0022377899007795 Published online by Cambridge University Press

We introduce the more general function

$$A_n(\lambda, z) = \mathscr{P} \int_{-v_m}^{v_m} dv \, \frac{v(v_m^2 - v^2)^{n-1}}{(\lambda - v^2)^{n+1}(v - z)}, \tag{A 2}$$

which satisfies

$$A_{n+1}(\lambda, z) = A_n(\lambda, z) + \frac{1 - v_m^2}{n+1} \frac{\partial}{\partial \lambda} A^n(\lambda, z), \tag{A 3}$$

$$A_1(\lambda, z) = \mathscr{P} \int_{-v_m}^{v_m} \frac{dv\, v}{(\lambda - v^2)^2 (v - z)} = -\frac{\partial}{\partial \lambda} L, \tag{A 4}$$

$$L = \mathscr{P} \int_{-v_m}^{v_m} \frac{dv\, v}{(\lambda - v^2)\,(v - z)} \frac{\lambda^{1/2}}{\lambda - z^2} \ln \left| \frac{\lambda^{1/2} - v_m}{\lambda^{1/2} + v_m} \right| + \frac{z}{\lambda - z^2} \ln \left| \frac{z - v_m}{z + v_m} \right|. \tag{A 5}$$

Equations (A 3)–(A 5) allow a recurrent calculation of $A_n(\lambda, z)$, from which the results required follow by setting $\lambda = 1$.

The RPDF (2.14) for $n = 3$ has the explicit form

$$\begin{aligned} z^2 W_3(v, z) = \frac{105(1 - v^2)^{3/2} z^2}{16 v^7} \Bigg\{ & \frac{v}{4(1 - z^2)} \left[5 - 9z^2 + v^2(3 + z^2) \right] - \frac{v}{2(1 - z^2)} \\ & + \frac{3 - 10z^2 + 15z^4 + 2v^2(1 - 6z^2 - 3z^4) + v^4(3 + 6z^2 - z^4)}{8\,(1 - z^2)^3} \ln \left(\frac{1 + v}{1 - v} \right) \\ & + \frac{z(v^2 - z^2)^2}{(1 - z^2)^3} \ln \left| \frac{v + z}{v - z} \right| \Bigg\}. \end{aligned} \tag{A 6}$$

References

Allen, M. C. and Melrose, D. B. 1982 Elliptically polarized modes in a pulsar magnetosphere *Proc. Astron. Soc. Aust.* **4**, 365–370.

Arons, J. and Barnard, J. J. 1986 Wave propagation in pulsar magnetospheres: dispersion relations and normal modes of plasmas in superstrong magnetic fields. *Astrophys. J.* **302**, 120–137.

Asséo, E. and Melikidze, G. I. 1998 Non-stationary pair plasma in a pulsar magnetosphere and the two-stream instability. *Mon. Not. R. Astron. Soc.* **301**, 59–71.

Asséo, E., Pellat, R. and Sol, H. 1983 Radiation or two-stream instability as a source of pulsar radio emission. *Astrophys. J.* **266**, 201–214.

Beskin, V. S., Gurevich, A. V. and Istomin, Ya. N. 1988 Theory of the radio emission of pulsars. *Astrophys. Space Sci.* **146**, 205–281.

Daugherty, J. K. and Harding, A. K. 1983 Pair production in superstrong magnetic fields. *Astrophys. J.* **273**, 761–773.

Gedalin, M. E. and Machabeli, G. Z. 1983 Oblique waves propagating in a relativistic electron-positron plasma. *Astrofizika* **19**, 153–159 (*Astrophysics* **19**, 91–95).

Gedalin, M., Melrose, D. B. and Gruman, E. 1998 Long waves in relativistic pair plasma in a strong magnetic field. *Phys. Rev.* **E57**, 3399–3410.

Godfrey, B. B., Shanahan, W. R. and Thode, L. E. 1975a Linear theory of a cold relativistic beam propagating along an external magnetic field. *Phys. Fluids* **18**, 346–355.

Godfrey, B. B., Newberger, B. S. and Taggart, K. A. 1975b A relativistic plasma dispersion function. *IEEE Trans. Plasma Sci.* **PS-3**, 60–67.

Hakim, R. and Mangeney, A. 1968 Relativistic kinetic equations including radiation effects. I. Vlasov approximation. *J. Math. Phys.* **9**, 116–130.

https://doi.org/10.1017/S0022377899007795 Published online by Cambridge University Press

Hardee, P. E. and Rose, W. K. 1976 A mechanism for the production of pulsar radio emission. *Astrophys. J.* **210**, 533–538.

Imre, K. 1962 Oscillations in a relativistic plasma. *Phys. Fluids* **5**, 459–466.

Kurşunoğlu, B. 1961 Relativistic plasma. *Nucl. Fusion* **1**, 213–223.

Lominadze, D. G. and Mikhailovskii, A. B. 1979 Longitudinal waves and two-stream instability in a relativistic plasma. *Zh. Eksp. Teor. Fiz.* **76**, 959–960 (*Soviet Phys. JETP* **49**, 483–487).

Lominadze, D. G., Mikhailovskii, A. B. and Sagdeev, R. Z. 1979 Langmuir turbulence of a relativistic plasma in a strong magnetic field. *Zh. Eksp. Teor Fiz.* **77**, 1951–1961 (*Soviet Phys. JETP* **50**, 927–932.

Lyutikov, M. 1998 Waves in a one-dimensional magnetized relativistic pair plasma. *Mon. Not. R. Astron. Soc.* **293**, 447–468.

Magneville, A. 1990 Plasma waves in hot relativistic beam–plasma systems. Part 1. Dispersion relations. *J. Plasma Phys.* **44**, 191–211.

Melrose, D. B. 1986 *Instabilities in Space and Laboratory Plasmas*. Cambridge University Press.

Melrose, D. B. and Stoneham, R. J. 1977 The natural modes in a pulsar magnetosphere. *Publ. Astron. Soc. Australia* **3**, 120–122.

Mikhailovskii, A. B., Onischenko, O. G., Suramlishvili, G. I. and Sharapov, S. E. 1982 The emergence of electromagnetic waves from pulsar magnetospheres. *Pis'ma Astrom. Zh.* **8**, 685–688 (*Soviet Astron. Lett.* **8**, 369–371).

Polyakov, A. 1983 A new kind of oscillations in a relativistic plasma. *Zh. Eksp. Teor. Fiz.* **85**, 1585–1589 (*Soviet Phys. JEPT* **58**, 922–924).

Prentice, A. J. R. 1967 Collective energy loss in relativistic plasmas. *Plasma Phys.* **9**, 433–455.

Ruderman, M. A. and Sutherland, P. G. 1975 Theory of pulsars: polar gaps, sparks, and coherent microwave radiation. *Astrophys. J.* **196**, 51–72.

Silin, V. P. 1960 On the electromagnetic properties of a relativistic plasma. *Zh. Eksp. Teor. Fiz.* **38**, 1577–1583 (*Soviet Phys. JEPT* **11**, 1136–1140).

Suvorov, E. V. and Chugunov, Yu. V. 1975 Electromagnetic waves in a relativistic plasma with a strong magnetic field. *Astrofizika* **11**, 305–318 (*Astrophysics* **11**, 203–211).

Trubnikov, B. A. 1958 Magnate emission of high temperature plasma. Thesis, Moscow Institute of Engineering and Physics (English translation in AEC-tr-4073, US Atomic Energy Commission, Oak Ridge, Tennessee, 1960).

Tsytovich, V. N. and Kaplan, S. A. 1972 Relativistic turbulence in pulsars. *Astrofizika* **8**, 441–460. (*Astrophysics* **8**, 260–272).

Volokitin, A. S., Krasnoselskikh, V. V. and Machabeli, G. Z. 1985 Waves in a relativistic electron–positron plasma in pulsar. *Soviet J. Plasma Phys.* **11**, 531–538.

von Hoensbroech, A., Lesch, H. and Kunzl, T. 1998 Natural polarization modes in pulsar magnetospheres. *Astron. Astrophys.* **336**, 209–219.

Weatherall, J. C. 1994 Streaming instability in relativistically hot pulsar magnetospheres. *Astrophys. J.* **428**, 261–266.

https://doi.org/10.1017/S0022377899007795 Published online by Cambridge University Press